

MoFM: A Large-Scale Human Motion Foundation Model

Mohammadreza Baharani
 The UNC at Charlotte
 Charlotte, NC
 mbaharan@charlotte.edu

Ghazal Alinezhad Noghre
 The UNC at Charlotte
 Charlotte, NC
 galinezh@charlotte.edu

Armin Danesh Pazho
 The UNC at Charlotte
 Charlotte, NC
 adaneshp@charlotte.edu

Gabriel Maldonado
 The UNC at Charlotte
 Charlotte, NC
 gmaldon2@charlotte.edu

Hamed Tabkhi
 The UNC at Charlotte
 Charlotte, NC
 htabkhiv@charlotte.edu

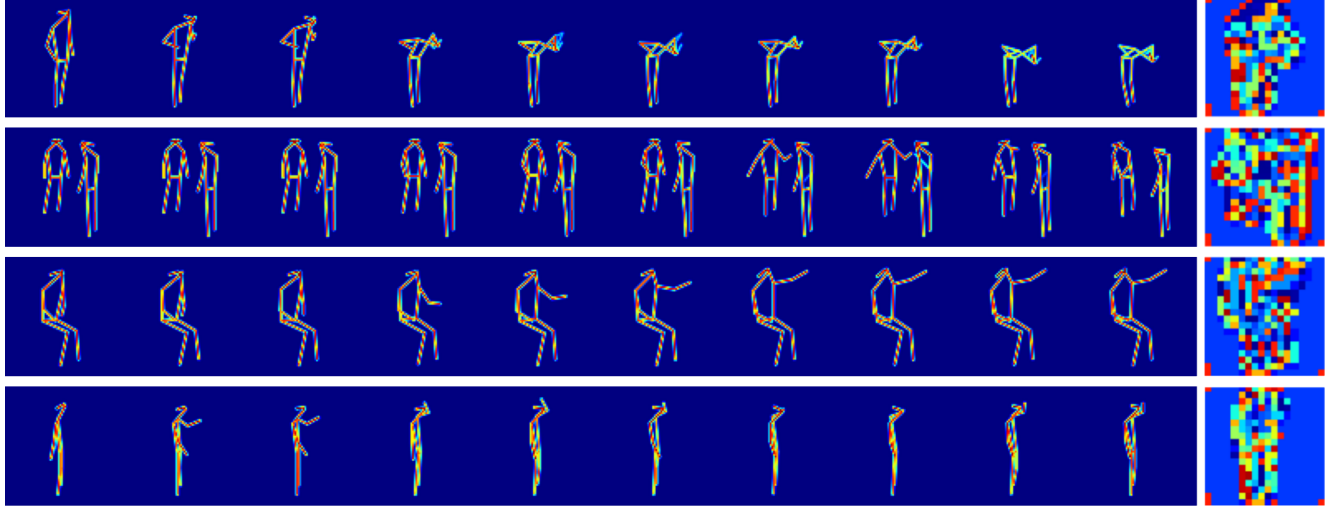


Figure 1. Visualization of videos with corresponding pose tokens normalized by vocabulary size. Each row shows skeletal motion frames alongside tokens, with values mapped from blue (low) to red (high), illustrating the alignment of skeletal actions with motion vocabulary.

Abstract

A Foundation Models (FM) have increasingly drawn the attention of researchers due to their scalability and generalization across diverse tasks. Inspired by the success of FMs and the principles that have driven advancements in Large Language Models (LLMs), we introduce MoFM as a novel Motion Foundation Model. MoFM is designed for the semantic understanding of complex human motions in

both time and space. To facilitate large-scale training, MotionBook, a comprehensive human motion dictionary of discretized motions is designed and employed. MotionBook utilizes Thermal Cubes to capture spatio-temporal motion heatmaps, applying principles from discrete variational models to encode human movements into discrete units for a more efficient and scalable representation. MoFM, trained on a large corpus of motion data, provides a foundational backbone adaptable to diverse downstream tasks, support-

ing paradigms such as one-shot, unsupervised, and supervised tasks. This versatility makes MoFM well-suited for a wide range of motion-based applications.

1. Introduction

Human-centric computer vision tasks such as pose estimation [16, 25, 86], action recognition [23, 27, 108], and anomaly detection [30, 69, 97] have garnered significant research attention. These tasks are pivotal in various applications, including surveillance systems [5, 67, 71] and healthcare monitoring [24, 37, 57].

Despite substantial progress, effectively capturing the complexity of human motion is a challenging endeavor due to the inherent variability in human poses, dynamic backgrounds, and the high dimensionality of visual data [4, 102]. To tackle these challenges, it is imperative to consider both optimization of the data modalities and development of advanced models capable of effectively understanding these data.

Utilizing the pixel data is a major approach in analyzing videos [73, 97, 110], which can be susceptible to background noise and biases introduced by visual contexts. A common strategy to simplify human motion analysis is to employ pose estimation techniques [16, 25, 86]. However, reducing raw pixel data to a sparse set of keypoints can lead to excessive abstraction and loss of valuable information such as fine-grained limb movements and contextual spatial relationships [23, 40]. Therefore, a balance must be struck between the high-dimensional raw pixel data and the overly abstracted keypoint representations. To address this issue, using heatmaps as the middle ground between pixels and poses is a well-known practice [26, 59]. Heatmaps, as the probable location of joints, preserve spatial uncertainty and provide a richer representation of human motion compared to discrete keypoints [23].

The emergence of Foundation Models (FMs) [15, 60, 94, 98] has revolutionized various AI domains, particularly in natural language processing with models like BERT [36], GPT-3 [10], and other Large Language Models (LLMs) [20, 66]. Such models have demonstrated remarkable scalability and generalization capabilities without extensive task-specific training. These models exhibit exceptional scalability and generalizability, without requiring extensive task-specific training. Consequently, FMs present a promising pathway for advancing human motion understanding.

Inspired by these advancements, we propose a novel Motion Foundation Model (MoFM) designed for the semantic understanding of complex human motions. Instead of processing entire videos or relying solely on keypoint-based poses, MoFM focuses on spatio-temporal heatmaps. To enable large-scale self-supervised training for human motion representation, we introduce a customized discrete Vari-

tional Encoder-Decoder (dVED), following principles from discrete Variational Autoencoders (dVAEs) [9, 87, 88]. Mapping motion heatmaps into Thermal Cubes, we then utilize the proposed dVED to encode them into a discrete latent representation (motion tokens as visualized in Fig. 1). This process creates the MotionBook dictionary, organizing human movements into discrete units. The encoder of dVED functions as a tokenizer to enable BERT-style [36] self-supervised MoFM backbone training through the masking of Thermal Cubes.

The MoFM backbone, trained on a large corpus of data, is designed to serve as a foundational model that can seamlessly adapt to diverse downstream tasks such as action classification and human anomaly detection. Rather than aiming to outperform existing state-of-the-art (SOTA) models, the MoFM backbone’s goal is to provide a flexible, task-agnostic foundation. Through minimal adjustments to the task-specific head, MoFM readily supports a range of applications, from one-shot learning scenarios to unsupervised and supervised tasks, underscoring its versatility for human motion analysis without the need for extensive retraining.

To assess the potential of the MoFM backbone, we target four human-centric downstream tasks: action recognition, one-shot action recognition, self-supervised anomaly detection, and supervised anomaly detection. For each task, we attach a simple, task-specific fully connected head to the MoFM backbone to establish a baseline. The results from this approach demonstrate MoFM’s effectiveness as a foundational model for motion-based applications.

Our experiments highlight its capacity to generalize across tasks, underscoring MoFM’s versatility as a comprehensive solution for diverse human motion understanding. The contributions of this paper are:

- A discrete Variational Encoder-Decoder (dVED) designed to encode Thermal Cubes into a discrete latent space (MotionBook) for structured human movement representation.
- Pose-aware self-supervised BERT-style training to apply masked Thermal Cubes for task-agnostic learning of human motion.
- Motion Foundation Model (MoFM) for semantic understanding of human motion, serving as foundational backbone for diverse downstream tasks.

2. Related Works

Various approaches have been proposed to address the challenges of understanding human motion, including pixel-based [8, 15, 97], keypoint/graph-based [80, 105, 106], and heatmap-based methods [23, 26]. Beyond these modalities, researchers have explored diverse model architectures to leverage them effectively, such as one-shot CNN-based methods [70, 77, 115], Graph Convolutional Networks (GCNs), and Transformers [3, 45, 99, 103, 112, 114].

Building on these representations, discrete Variational Autoencoders (dVAEs) [33, 72, 74, 89] have been developed to capture low-frequency image structures by constructing a quantized latent space. This latent encoding has enabled the use of dVAE encoders for training transformers to learn joint distributions between text and images [72] and to model spatial correlations between image patches [7, 22]. These self-supervised transformers can then be fine-tuned for tasks such as image classification and object localization.

Building on these advancements, our work leverages the strengths of foundational models and discrete representation learning to address the unique challenges in human motion understanding. By combining the generalization of transformer with the structured representations of discrete variational encoders, our Motion Foundation Model (MoFM) introduces a self-supervised approach that captures both the spatio-temporal granularity of motion heatmaps and the interpretability of discrete motion tokens. This approach enables MoFM to generalize effectively across various human motion tasks, establishing it as a versatile backbone for applications such as action recognition and anomaly detection.

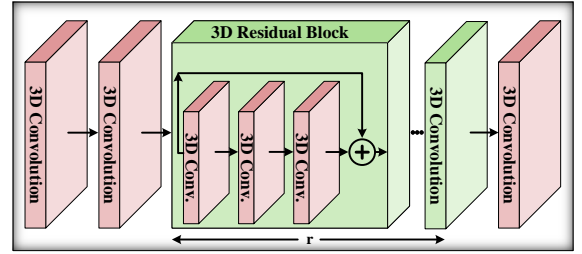
Foundation models have revolutionized natural language processing (NLP) and computer vision through large-scale pretraining and self-supervised learning, achieving remarkable generalization capabilities and enabling easy fine-tuning for domain-specific tasks [10, 21, 66]. In NLP, models such as BERT [21], GPT-3 [10], and K2 [20] have demonstrated the effectiveness of training on unlabeled data to capture context and language nuances. Furthermore, transformer architectures with attention mechanisms [22, 91] have been integral to the success of foundational models across tasks.

In computer vision, foundation models [12, 39] have adapted these principles to address complex visual tasks. They leverage masked image modeling [6], vision transformers [22], and extensive datasets to learn meaningful visual representations.

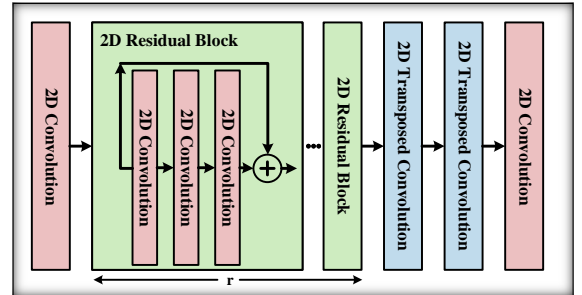
3. Problem Formulation

The objective of this work is to develop a robust foundational model, MoFM, that learns the semantics of human motion using representations called thermal cubes and pose tokens, enabling an efficient and generalized understanding of human motion for downstream tasks. This process begins by constructing a spatio-temporal heatmap, U , for a sequence of F frames in the 2D pose skeleton $P = \{P_i\}_{i=0}^{F-1}$. Subsequently, U is divided into Thermal Cubes, denoted as $C = \{C_i\}_{i=0}^{K-1}$, where K represents the number of tokens MoFM backbone can process simultaneously.

To facilitate self-supervised training, we first employ the Thermal Cubes C to train a dVED, generating a “Motion-



(a) dVED Encoder.



(b) dVED Decoder.

Figure 2. Architecture of the proposed custom dVED encoder and decoder. The variable r represents the number of layers in which the 2D/3D residual block can be repeated.

Book” vocabulary \mathcal{V} . With the vocabulary size configured as the transformer head (T-Head) dimension and applying pose-aware BERT-style masked modeling, we train the task-agnostic MoFM backbone to capture motion semantics across tokens. Subsequently, the pretrained MoFM backbone serves as encoder for downstream applications. Fig. 4 illustrates this framework, with detailed steps provided in the following sections.

4. MoFM

4.1. Spatio-Temporal Pose Representation

Given an input sequence of 2D skeleton keypoints across F frames for J joints, our initial step involves creating a spatio-temporal heatmap. This is achieved by implementing J Gaussian functions across the F frames as follows:

$$U_f = e^{-\frac{(i-x_{jf})^2 + (i-y_{jf})^2}{2 \times \sigma^2}}, \quad (1)$$

where σ is responsible for determining the spread of the energy around each joint, labeled as j , located at coordinates $\langle x_{jf}, y_{jf} \rangle$ for the frame f . A max-pooling filter, spanning over J joints, is applied to the thermal energy matrix $U|U \in \mathbb{R}^{J \times F \times H \times W}$, where H and W are the height

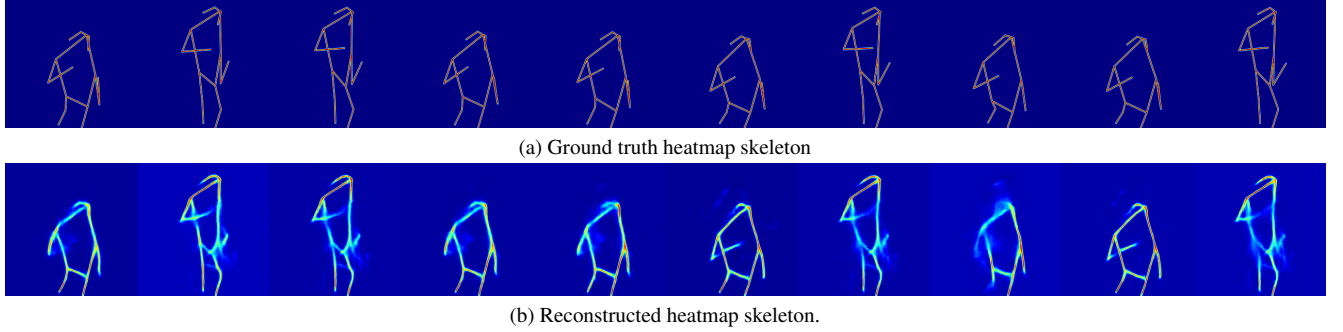


Figure 3. Comparison of heatmap skeletons: (a) Ground truth heatmap skeleton used as input for dVED; (b) Reconstructed heatmap skeleton generated by dVED. A ghosting effect is observed for moving joints in the dVED output.

and the width of the heatmap, respectively. This operation condenses U into a matrix of reduced dimensions U_R , where $U_R \in \mathbb{R}^{F \times H \times W}$. This technique simplifies the representation of thermal energy across frames by emphasizing the most significant energy values in each region of the heatmap. Both U and U_R are subsequently utilized for training the dVED.

4.1.1. Thermal Cubes

To configure the data for processing by a transformer (MoFM backbone), the thermal matrix U must be segmented into multiple cubes, capturing both the spatial and temporal dimensions of the motion. Thus, U is transformed into $K = \frac{HW}{D_S \times D_S}$ cubes, where each cube $C_i \in \mathbb{R}^{J \times F \times D_S^2}$ and D_S is the patch size. In this work, we centered and scaled the skeleton to fit a heatmap size of $H = W = 72$. The skeleton structure has $J = 17$ joints, and $F = 48$. We also set D_S to 4, resulting in the thermal matrix U being divided into $K = 324$ cubes, each with the shape $C_i \in \mathbb{R}^{17 \times 48 \times 4 \times 4}$.

4.1.2. Motion Tokens

To enable masked input self-supervised training of a transformer, we first need to convert thermal cubes into discrete tokens. Following the methodology outlined by [33, 72], we employ a custom discrete Variational Encoder-Decoder (dVED) to facilitate the mapping function $\mathcal{G} : U \rightarrow \widehat{U}_R$:

$$\widehat{U}_R = f_{\text{dec}}(f_{\text{GS}}(f_{\text{enc}}(U; \theta), \tau); \phi), \quad (2)$$

where θ and ϕ represent the encoder and decoder learnable parameters, respectively, and τ is the Gumbel-Softmax temperature parameter. The encoder, Gumbel-Softmax approximation, and decoder are represented by f_{enc} , f_{GS} , and f_{dec} , respectively. Formally, the encoder component of the dVED, which functions as a tokenizer, converts the initial heatmap, $C = \{C_i\}_{i=0}^{K-1}$, into K discrete tokens, denoted as $z = \{z_i\}_{i=0}^{K-1}$. Each z_i is a categorical variable with class probabilities $\pi = \{\pi_i\}_{i=0}^{T-1}$. T indicates the size of the

vocabulary. Using the Gumbel-Softmax trick, we have:

$$z_i = \text{one_hot}(\text{argmax}_i [g_i + \log \pi_i]), \quad (3)$$

where $g = \{g_i\}_{i=0}^{T-1}$ are samples drawn from $\text{Gumbel}(0, 1)$ ¹. The vocabulary, \mathcal{V} , is constructed as a MotionBook and is defined by the following matrix:

$$\mathcal{V} = \begin{pmatrix} v_{0,0} & v_{1,1} & \cdots & v_{0,D-1} \\ \vdots & \vdots & \ddots & \vdots \\ v_{T-1,0} & v_{T-1,1} & \cdots & v_{T-1,D-1} \end{pmatrix}, \quad (4)$$

where D denotes the dimensionality of each vocabulary entry. The motion dictionaries are trained and later used by the decoder to reconstruct \widehat{U}_R .

4.2. dVED for Motion Discretization

In this paper, we present a custom dVED model with distinct encoder and decoder structures. The encoder utilizes 3D ResBlocks and 3D convolution blocks for dimensionality reduction, while the decoder employs 2D transposed convolutions and 2D ResBlocks to reconstruct inputs from the MotionBook back to U_R as illustrated in Fig. 2.

The encoder, $q_\theta(z|U)$, is trained to map thermal cubes to a discrete latent space, z , while the decoder reconstructs the condensed heatmap, U_R , by applying $p_\phi(U_R|z)$. Therefore, The objective function can be formalized as follows:

$$\mathcal{L} = -\mathbb{E}_{q_\theta(z|U)} [\log p_\phi(U_R|z)] + \beta \times D_{\text{KL}}(q_\theta(z|U) \parallel p(z)) \quad (5)$$

where $\log p_\phi(U_R|z)$ represents the likelihood of the reconstructed data given the latent variables, D_{KL} is the KL divergence between the approximate posterior $q_\theta(z|U)$ and

¹The random variable g distributed as $\text{Gumbel}(0, 1)$ can be generated by $g = -\log(-\log(u))$, where u is drawn from a uniform distribution, $u \sim U(0, 1)$. Alternatively, it is also common to use exponential distribution sampling, where $g = -\log(x)$, and $x \sim \text{Exp}(\lambda)$ is drawn from an exponential distribution with a rate parameter $\lambda = 1$.

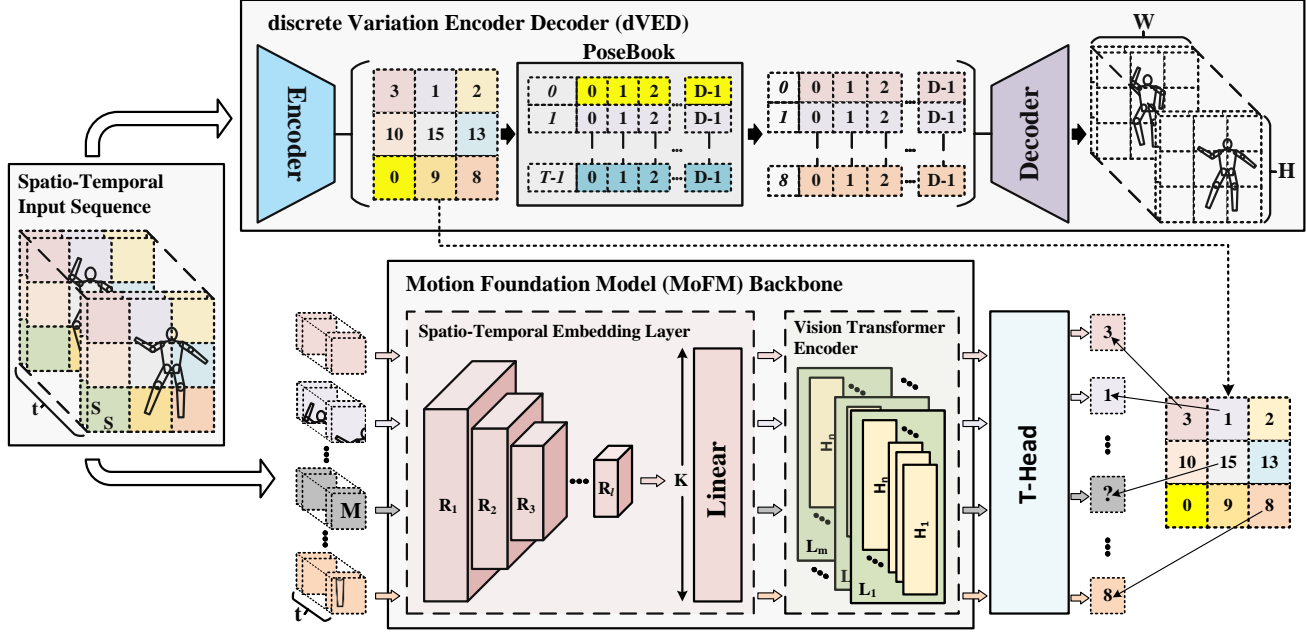


Figure 4. Overview of Motion Foundation Model (MoFM). Poses are converted into heatmap representations using a Gaussian function (Eq. (1)), producing a series of thermal cubes. Before pre-training, we train the custom dVED model for reconstruction. This involves tokenizing a series of heatmap cubes in both spatial and temporal dimensions according to a learned vocabulary. After cubing, tokens are masked keypoint-wise with a special mask embedding [M]. The resulting $\{C_i^m\}_{i=0}^{K-1}$ masked cubes are then fed into a vision transformer encoder. The backbone predicts the visual tokens of the discretized image based on $\{z_i\}_{i=0}^{K-1}$ generated by dVED.

the prior $p(z)$, typically chosen to be uniform over the discrete categories, and β is the coefficient for the KL divergence term.

The Gumbel-Softmax trick allows this objective to be optimized via gradient descent by approximating categorical sampling using the softmax function:

$$y_i = \frac{\exp((\log(\pi_i) + g_i)/\tau)}{\sum_{j=0}^{T-1} \exp((\log(\pi_j) + g_j)/\tau)}, \quad (6)$$

where τ is the temperature that controls the softness of the distribution. We schedule τ to be dynamically reduced during the training phase to improve performance. For our setup, we approximate the reconstruction term $\mathbb{E}_{q_\theta(z|U)}[\log p_\phi(U_R|z)]$ with the smooth L1 loss function.

For better generalization of dVED, it is essential that the poses encompass a wide variety of actions covering the full range of motion. We chose the CMU Panoptic dataset, a comprehensive collection offering sequences of pose information from multiple perspectives. For each randomly selected video from the dataset, we divided it into F bins and randomly selected a frame from each bin. We then applied Eq. (1) to generate U , and U_R . The dVED model architecture features an encoder with two 3D Convolution and two 3D ResNet blocks, and a decoder with two 2D Convolution and two 2D ResNet blocks, with a hidden dimension of

256. The pose book also has a 256 hidden dimension and a vocabulary size of 8192. Training was performed over 20 epochs with a batch size of 24, utilizing the AdamW optimizer and a WarmupCosineLR scheduler. The maximum and minimum learning rates were set to $3.0e-4$ and $1.0e-6$, respectively, with a single warmup epoch. Fig. 3 qualitatively compares the performance of dVED, shown in Fig. 3b, with the ground truth, shown in Fig. 3a. A notable phenomenon observed in the reconstructed heatmap is the ghosting effect around moving joints, which clearly demonstrates how the thermal energy transitions from one point to another in the direction of movement.

4.3. MoFM Backbone and Self-supervised Training

The Spatio-Temporal Embedding Layer of the MoFM consists of l layers of 3D residual block (R) to map C to $\mathcal{H}|\mathcal{H} \in \mathbb{R}^{K \times H}$ where H is the hidden size of the vision transformer encoder. The transformer encoder used in our work is the base transformer model proposed in [22, 90]. The architecture uses 12 layers and 12 attention heads, each with a size of 64. The hidden dimension, feed-forward network size, and maximum sequence length are set to 768, 3072, and 384, respectively.

After training dVED, we used its encoder as a tokenizer. As outlined in Sec. 4.1.2, to enable self-supervised train-

ing of the transformer encoder, we split the input U into K cubes, $\{C_i\}_{i=0}^{K-1}$, and utilized the dVED tokenizer to map these cubes to the latent space, $\{z_i\}_{i=0}^{K-1}$. Consequently, we set the transformer’s input sequence length to K .

We propose a targeted approach for motion-wise masking of spatio-temporal cubes, detailed in Algorithm 1. Initially, we experimented with blockwise masking as suggested in [7]; however, while this reduced the loss error, it did not yield qualitatively accurate reconstructions. We attribute this to the random block placements, which often masked regions without any pose skeletons, leading to ineffective learning. To address this, we developed keypoint-wise masking. In this approach, we randomly select a joint j from the given set P . For each selected joint j , located at coordinates $\langle x_{jf}, y_{jf} \rangle$ in frame f , we identify the block containing the joint and mark it as a candidate for masking. This process is repeated until the number of masked blocks specified by `num_block_to_mask` in Algorithm 1 is reached.

The transformer encoder is then trained to classify the received Thermal Cubes based on the output of the dVED encoder. Fig. 4 illustrates the closed-loop training process, in which the dVED encoder functions as a tokenizer to support self-supervised training. Masked cubes, represented as [M], are shaded in gray and treated as learnable parameters. Training was conducted over 20 epochs with a batch size of 32, using the AdamW optimizer with a cosine learning rate scheduler and warmup. The learning rate was set between a maximum of 1.5×10^{-4} and a minimum of 1.0×10^{-8} , with a single warmup epoch.

5. Experimental Results

This section presents experimental results to demonstrate the capabilities of the pretrained MoFM when used as a backbone for various downstream tasks. While MoFM is applicable to a wide range of applications, we have selected DT1: action classification, DT2: one-shot action classification, DT3: self-supervised human anomaly detection, and DT4: supervised human anomaly detection to showcase its versatility. In all these tasks, we have only added a basic fully connected linear head on top of MoFM to form a simple baseline.

All training used six NVIDIA A6000 GPUs. Other experimental setup and hyper parameters for each downstream task are fully explained in the supplementary material.

5.1. DT1: Action Classification

We explore the potential of MoFM’s pretrained human motion representations as a backbone for learning action semantics. For this, we utilize the NTU-RGB+D [78] dataset, containing 57K videos across 60 action classes, following the Cross-Subject (X-Sub) and Cross-View (X-View) splits. We also leverage the extended NTU-RGB+D-120

[51] dataset, which includes 114K videos covering 120 action classes with Cross-Subject (X-Sub) and Cross-Setup (X-Set) splits. For both datasets, we extract 2D skeletons using HRNet [85] as described in [23]. As shown in Tab. 1 and Tab. 2, our methods achieve performance on par with or surpassing SOTA approaches, underscoring MoFM’s capability to generalize effectively to the downstream task of human action recognition.

Table 1. Fine-tuning results for action classification as the downstream task on NTU RGB+D [78] dataset (top-1% accuracy). MoFM-FC represents MoFM with a basic fully connected head to serve as a simple baseline.

Method	Source	X-Sub	X-View
Vemulapalli et al. [92]	CVPR	50.1	52.8
Liu et al. [46]	ECCV	69.2	77.7
Soo et al. [83]	CVPR	74.3	83.1
Zhang et al. [113]	ICCV	79.2	87.7
Li et al. [44]	CVPR	81.8	88.0
Cho et al. [19]	WACV	87.2	92.7
Li et al. [43]	CVPR	86.8	94.2
Song et al. [82]	TCSVT	87.3	93.6
Shi et al. [80]	CVPR	88.5	95.1
Shi et al. [79]	CVPR	89.2	95.5
Chen et al. [14]	AAAI	91.5	96.6
Miao et al. [64]	TCSVT	90.9	96.6
Xia et al. [101]	TMM	87.1	93.2
Jang et al. [34]	TCSVT	92.7	96.9
Liu et al. [55]	CVPR	91.5	96.2
Li et al. [42]	CVPR	86.2	92.5
Shi et al. [81]	CVPR	88.5	95.1
Duan et al. [23]	CVPR	93.1	95.7
Su et al. [84]	ICCV	89.7	96.3
Yan et al. [104]	AAAI	81.5	88.3
Yang et al. [107]	ICCV	88.0	94.9
Cheng et al. [17]	CVPR	90.7	96.5
MoFM-FC (Ours)	-	89.4	94.7

5.2. DT2: One-shot Action Classification

We further assess MoFM’s capability in recognizing one-shot actions by adding a fully connected layer that embeds the given action onto a δ -dimensional hypersphere, where $\delta = 2048$ for this experiment. Following NTU-RGB+D-120 [51] guidelines, we trained the model on an *auxiliary set* of 100 labeled samples using supervised contrastive learning [38]. In each batch, m samples of the same class were randomly selected from the auxiliary set, and a supervised contrastive loss was applied to cluster samples of the same class while separating samples of different classes. Evaluation was conducted by calculating cosine similarity

Algorithm 1 Generate Mask from Keypoints

Input : KP : array of shape $(F \times J, 2)$ containing coordinate of keypoints in $[x, y]$
 H : Height of the original heatmap
 W : Width of the original heatmap
 D_S : Size of spatial resolution
 min_masked_number : Minimum number of points to be randomly selected for masking
 max_masked_number : Maximum number of points to be randomly selected for masking

Output: $final_mask$: A single mask of shape $(total_rows_squares, total_cols_squares)$ with 1s where squares are masked

```
total_rows_squares ←  $\lfloor \frac{H}{D_S} \rfloor + (1 \text{ if } H \% D_S \text{ else } 0)$ 
total_cols_squares ←  $\lfloor \frac{W}{D_S} \rfloor + (1 \text{ if } W \% D_S \text{ else } 0)$ 
final_mask ← zeros((total_rows_squares, total_cols_squares))
total_points ←  $F \times J$ 
α ← max(1, min(min_masked_number, total_points))
β ← min(max_masked_number, total_points)
num_block_to_mask ← RandomSample({α, α + 1, ..., β, β + 1}, 1)
selected_indices ← RandomSample({0, 1, 2, ..., total_points - 1}, num_block_to_mask)
selected_points ←  $KP[selected\_indices]$ 
foreach  $(x, y) \in selected\_points$  do
     $col \leftarrow \left\lfloor \frac{x}{D_S} \right\rfloor$ 
     $row \leftarrow \left\lfloor \frac{y}{D_S} \right\rfloor$ 
    if  $0 \leq row < total\_rows\_squares$  and  $0 \leq col < total\_cols\_squares$  then
        |  $final\_mask[row, col] \leftarrow 1$ 
    end
end
return  $final\_mask$ 
```

between the test set and 20 exemplars for each remaining class. Tab. 3 presents the accuracy comparison of MoFM with recent approaches, demonstrating MoFM’s effectiveness in handling one-shot action classification, similar to the DT1 experiments.

5.3. DT-3: Self-supervised Human Anomaly Detection

In self-supervised human video anomaly detection, the objective is to enable models to discern patterns of typical human behavior and identify deviations as anomalous [54]. Self-supervised methods typically formulate proxy tasks, such as reconstruction [65] or future prediction [65, 75, 111], training the model exclusively on normal data. This encourages the model to internalize the underlying dynamics of normal human motion. During inference, the model’s ability to perform these tasks serves as an indicator of abnormality detection.

Inspired by [93], we define a self-supervised jigsaw puzzle task at the token level, rather than at the pixel level as in [93]. A simple fully connected layer with 12 neurons is added as the task head. Tokens are grouped into 12 puzzle pieces, which are shuffled during training, and the network is fine-tuned with multi-label supervision using cross-

entropy loss to predict the correct positions of the pieces. During inference, no shuffling occurs; instead, the model’s predictions are used to compute a normality score. For abnormal behavior, prediction accuracy declines, resulting in a non-diagonal probability matrix. The lowest probability along the diagonal is taken as the normality score. If multiple individuals are present in the scene, the frame’s overall normality score is determined by the minimum of their individual scores.

To evaluate our model, we use the widely adopted ShanghaiTech Campus (SHT) dataset [53]. Following previous SOTA methods [30, 61, 109], we use AlphaPose [41] for pose extraction and tracking to ensure fair comparison. We also report results on the Human-Related SHT subset [65], which focuses exclusively on human activities. We report results in terms of frame level Area Under the Receiver Operating Characteristic Curve (AUC-ROC).

As shown in Tab. 4, MoFM-FC achieves an AUC-ROC of 76.56% on SHT [53] and 77.26% on HR-SHT [65], demonstrating performance comparable to other SOTA models. These results underscore the adaptability and versatility of the MoFM as a backbone, demonstrating that with the addition of a simple linear head, it can be effectively utilized for self-supervised anomaly detection.

Table 2. Fine-tuning results for action classification as the downstream task on NTU RGB+D 120 [51] dataset (top-1% accuracy). MoFM-FC represents MoFM with a basic fully connected head to serve as a simple baseline.

Methods	Source	X-Sub	X-Set
Yan et al. [104]	AAAI	70.7	73.2
Li et al. [43]	CVPR	77.7	78.9
Song et al. [82]	TCSVT	81.1	82.7
Shi et al. [80]	CVPR	82.9	84.9
Liu et al. [55]	CVPR	86.9	88.4
Chen et al. [14]	AAAI	87.5	88.8
Miao et al. [64]	TCSVT	86.3	87.8
Wu et al. [100]	TCSVT	86.0	87.6
Xia et al. [101]	TMM	81.0	82.2
Jang et al. [34]	TCSVT	88.9	90.6
Liu et al. [48]	CVPR	67.7	66.9
Ke et al. [35]	TIP	62.2	61.8
Shahroudy et al. [78]	CVPR	25.5	26.3
Liu et al. [46]	ECCV	55.7	57.9
Caetano et al. [11]	SIBGRAPI	67.9	62.8
Cheng et al. [17]	CVPR	80.9	83.2
MoFM-FC (Ours)	-	78.0	83.7

Table 3. Fine-tuning results for one-shot action classification as the downstream task on NTU RGB+D 120 [51] dataset. MoFM-FC represents MoFM with a basic fully connected head to serve as a simple baseline.

Methods	Source	Top-1%
Liu et al. [49]	CVPR	41.0
Liu et al. [49]	CVPR	42.1
Liu et al. [47]	TPAMI	42.9
Liu et al. [50]	TPAMI	45.3
Sabater et al. [76]	CVPR	46.5
Memmesheimer et al. [62]	ICPR	50.9
Memmesheimer et al. [63]	WACV	54.2
Wang et al. [96]	ECCV	49.0
Wang et al. [95]	ACCV	57.0
Zhu et al. [116]	WACV	57.6
MoFM-FC (Ours)	-	56.6

5.4. DT4: Supervised Human Anomaly Detection

In supervised human anomaly detection, the task is framed as a binary classification problem. Similar to previous downstream tasks, we add a fully connected layer as the head. During inference, the probability assigned to the normal class serves as the normality score. In line with the self-supervised approach, if multiple individuals are present, the frame’s overall normality score is determined by the mini-

Table 4. Fine-tuning results for self-supervised human anomaly detection as the downstream task on ShanghaiTech Campus (SHT) [53] and HR-ShanghaiTech (HR-SHT) [65] datasets (AUC-ROC%). MoFM-FC represents MoFM with a basic fully connected head to serve as a simple baseline.

Methods	Source	SHT	HR-SHT
Wang et al. [97]	PR	71.30	-
Zaheer et al. [110]	CVPR	78.93	-
Luo et al. [58]	ICCV	68.00	-
Abati et al. [1]	CVPR	72.50	-
Hasan et al. [29]	CVPR	70.40	69.80
Liu et al. [52]	CVPR	72.80	72.70
Morais et al. [65]	CVPR	73.40	75.40
Markovitz et al. [61]	CVPR	75.50	-
Jain et al. [32]	ICPR	74.90	75.70
Chen et al. [13]	JVCIR	75.90	-
Rodrigues et al. [75]	WACV	76.03	77.04
Huang et al. [31]	CVPR	82.90	86.97
Noghere et al. [68]	WACV	80.67	81.77
MoFM-FC (Ours)	-	76.56	77.26

mum of their individual scores.

Table 5. Fine-tuning results for supervised human anomaly detection as the downstream task on the UBnormal [2] dataset (AUC%). MoFM-FC represents MoFM with a basic fully connected head to serve as a simple baseline.

Methods	Source	AUC-ROC%
Georgescu et al. [28]	TPAMI	61.3
Bertasius et al. [8]	ICML	68.5
Yan et al. [105]	AAAI	78.1
Shi et al. [80]	CVPR	74.1
Cheng et al. [18]	CVPR	64.6
Liu et al. [56]	CVPR	77.8
MoFM-FC (Ours)	-	69.55

For evaluation, we utilize the UBnormal dataset [2] and measure the model’s performance using frame-level AUC-ROC, consistent with prior SOTA approaches [8, 18, 28, 30, 56, 80, 105]. To address data imbalance in the training set, we apply data augmentation techniques, including random scaling, jitter noise, and horizontal flipping, to increase the representation of abnormal samples. Additionally, we use a weighted cross-entropy loss, giving 2× greater weight to abnormal samples to further mitigate class imbalance.

Tab. 5 demonstrates the effectiveness of MoFM-FC compared to other SOTA models. Our model achieves an AUC-ROC of 69.55%, showing performance comparable to other models and highlighting the capability of the MoFM backbone for supervised anomaly detection.

6. Conclusion

In this work we presented MoFM, a large-scale motion foundation model that understands the semantics of human motions. By utilizing Thermal Cubes and a discrete Variational Encoder-Decoder (dVED) model, we mapped spatio-temporal heatmaps into a discrete latent space, creating the comprehensive MotionBook dictionary. This approach enables task-agnostic self-supervised training, allowing MoFM to learn rich representations of human motion. Using MoFM as a foundational backbone, augmented with a simple fully connected linear layer to create a baseline, we have demonstrated its capabilities in handling downstream tasks including action classification, one-shot action classification, self-supervised human anomaly detection, and supervised human anomaly detection. We believe that MoFM will serve as a valuable foundation for future research endeavors in human motion understanding, enabling the development of more advanced models and applications in the field.

References

[1] Davide Abati, Angelo Porrello, Simone Calderara, and Rita Cucchiara. Latent space autoregression for novelty detection. In *Proceedings of the IEEE/CVF conference on computer vision and pattern recognition*, pages 481–490, 2019. 8

[2] Andra Acsintoa, Andrei Florescu, Mariana-Iuliana Georgescu, Tudor Mare, Paul Sumedrea, Radu Tudor Ionescu, Fahad Shahbaz Khan, and Mubarak Shah. Ub-normal: New benchmark for supervised open-set video anomaly detection. In *Proceedings of the IEEE/CVF Conference on Computer Vision and Pattern Recognition (CVPR)*, 2022. 8, 1

[3] Dasom Ahn, Sangwon Kim, Hyunsu Hong, and Byoung Chul Ko. Star-transformer: A spatio-temporal cross attention transformer for human action recognition. In *2023 IEEE/CVF Winter Conference on Applications of Computer Vision (WACV)*, pages 3319–3328, 2023. 2

[4] Ghazal Alinezhad Noghre, Armin Danesh Pazho, Vinit Katariya, and Hamed Tabkhi. Understanding the challenges and opportunities of pose-based anomaly detection. In *Proceedings of the 8th international Workshop on Sensor-Based Activity Recognition and Artificial Intelligence*, pages 1–9, 2023. 2

[5] Babak Rahimi Ardabili, Armin Danesh Pazho, Ghazal Alinezhad Noghre, Christopher Neff, Sai Datta Bhaskararayuni, Arun Ravindran, Shannon Reid, and Hamed Tabkhi. Understanding policy and technical aspects of ai-enabled smart video surveillance to address public safety. *Computational Urban Science*, 3(1):21, 2023. 2

[6] Hangbo Bao, Li Dong, and Furu Wei. BEiT: BERT pre-training of image transformers. In *International Conference on Learning Representations*, 2021. 3

[7] Hangbo Bao, Li Dong, Songhao Piao, and Furu Wei. BEiT: BERT pre-training of image transformers. In *International Conference on Learning Representations*, 2022. 3, 6

[8] Gedas Bertasius, Heng Wang, and Lorenzo Torresani. Is space-time attention all you need for video understanding? In *ICML*, page 4, 2021. 2, 8

[9] Biswajit Biswas, Swarup Kr Ghosh, and Anupam Ghosh. Dvae: deep variational auto-encoders for denoising retinal fundus image. *Hybrid machine intelligence for medical image analysis*, pages 257–273, 2020. 2

[10] Tom B Brown. Language models are few-shot learners. *arXiv preprint arXiv:2005.14165*, 2020. 2, 3

[11] C. Caetano, F. Bremond, and W. Schwartz. Skeleton image representation for 3d action recognition based on tree structure and reference joints. In *2019 32nd SIBGRAPI Conference on Graphics, Patterns and Images (SIBGRAPI)*, pages 16–23, Los Alamitos, CA, USA, 2019. IEEE Computer Society. 8

[12] K. Chen et al. InternVL: Vision-language pretraining with large-scale data. *arXiv preprint arXiv:2201.00000*, 2022. 3

[13] Xiaoyu Chen, Shichao Kan, Fanghui Zhang, Yigang Cen, Linna Zhang, and Damin Zhang. Multiscale spatial temporal attention graph convolution network for skeleton-based anomaly behavior detection. *Journal of Visual Communication and Image Representation*, 90:103707, 2023. 8

[14] Zhan Chen, Sicheng Li, Bing Yang, Qinghan Li, and Hong Liu. Multi-scale spatial temporal graph convolutional network for skeleton-based action recognition. In *Proceedings of the AAAI conference on artificial intelligence*, pages 1113–1122, 2021. 6, 8

[15] Zhe Chen, Jiannan Wu, Wenhui Wang, Weijie Su, Guo Chen, Sen Xing, Muyan Zhong, Qinglong Zhang, Xizhou Zhu, Lewei Lu, et al. Internvl: Scaling up vision foundation models and aligning for generic visual-linguistic tasks. In *Proceedings of the IEEE/CVF Conference on Computer Vision and Pattern Recognition*, pages 24185–24198, 2024. 2

[16] Bowen Cheng, Bin Xiao, Jingdong Wang, Honghui Shi, Thomas S Huang, and Lei Zhang. Higherhrnet: Scale-aware representation learning for bottom-up human pose estimation. In *Proceedings of the IEEE/CVF conference on computer vision and pattern recognition*, pages 5386–5395, 2020. 2

[17] Ke Cheng, Yifan Zhang, Xiangyu He, Weihan Chen, Jian Cheng, and Hanqing Lu. Skeleton-based action recognition with shift graph convolutional network. In *2020 IEEE/CVF Conference on Computer Vision and Pattern Recognition (CVPR)*, pages 180–189, 2020. 6, 8

[18] Ke Cheng, Yifan Zhang, Xiangyu He, Weihan Chen, Jian Cheng, and Hanqing Lu. Skeleton-based action recognition with shift graph convolutional network. In *Proceedings of the IEEE/CVF conference on computer vision and pattern recognition*, pages 183–192, 2020. 8

[19] Sangwoo Cho, Muhammad Maqbool, Fei Liu, and Hassan Foroosh. Self-attention network for skeleton-based human action recognition. In *Proceedings of the IEEE/CVF winter conference on applications of computer vision*, pages 635–644, 2020. 6

[20] Cheng Deng, Tianhang Zhang, Zhongmou He, Qiyuan Chen, Yuanyuan Shi, Yi Xu, Luoyi Fu, Weinan Zhang, Xining Wang, Chenghu Zhou, et al. K2: A foundation language model for geoscience knowledge understanding and utilization. In *Proceedings of the 17th ACM International Conference on Web Search and Data Mining*, pages 161–170, 2024. 2, 3

[21] Jacob Devlin, Ming-Wei Chang, Kenton Lee, and Kristina Toutanova. Bert: Pre-training of deep bidirectional transformers for language understanding. In *North American Chapter of the Association for Computational Linguistics*, 2019. 3

[22] Alexey Dosovitskiy, Lucas Beyer, Alexander Kolesnikov, Dirk Weissenborn, Xiaohua Zhai, Thomas Unterthiner, Mostafa Dehghani, Matthias Minderer, Georg Heigold, Sylvain Gelly, Jakob Uszkoreit, and Neil Houlsby. An image is worth 16x16 words: Transformers for image recognition at scale. In *International Conference on Learning Representations*, 2021. 3, 5

[23] Haodong Duan, Yue Zhao, Kai Chen, Dahua Lin, and Bo Dai. Revisiting skeleton-based action recognition. In *2022 IEEE/CVF Conference on Computer Vision and Pattern Recognition (CVPR)*, pages 2959–2968, 2022. 2, 6

[24] Ushaa Eswaran and Alex Khang. Artificial intelligence (ai)-aided computer vision (cv) in healthcare system. In *Computer Vision and AI-Integrated IoT Technologies in the Medical Ecosystem*, pages 125–137. CRC Press, 2024. 2

[25] Hao-Shu Fang, Jiefeng Li, Hongyang Tang, Chao Xu, Haoyi Zhu, Yuliang Xiu, Yong-Lu Li, and Cewu Lu. Alphapose: Whole-body regional multi-person pose estimation and tracking in real-time. *IEEE Transactions on Pattern Analysis and Machine Intelligence*, 45(6):7157–7173, 2022. 2

[26] Runyang Feng, Yixing Gao, Tze Ho Edden Tse, Xueqing Ma, and Hyung Jin Chang. Diffpose: Spatiotemporal diffusion model for video-based human pose estimation. In *Proceedings of the IEEE/CVF International Conference on Computer Vision*, pages 14861–14872, 2023. 2

[27] Pei Geng, Xuequan Lu, Chunyu Hu, Hong Liu, and Lei Lyu. Focusing fine-grained action by self-attention-enhanced graph neural networks with contrastive learning. *IEEE Transactions on Circuits and Systems for Video Technology*, 33(9):4754–4768, 2023. 2

[28] Mariana Iuliana Georgescu, Radu Tudor Ionescu, Fa-had Shahbaz Khan, Marius Popescu, and Mubarak Shah. A background-agnostic framework with adversarial training for abnormal event detection in video. *IEEE transactions on pattern analysis and machine intelligence*, 44(9):4505–4523, 2021. 8

[29] Mahmudul Hasan, Jonghyun Choi, Jan Neumann, Amit K Roy-Chowdhury, and Larry S Davis. Learning temporal regularity in video sequences. In *Proceedings of the IEEE conference on computer vision and pattern recognition*, pages 733–742, 2016. 8

[30] Or Hirschorn and Shai Avidan. Normalizing flows for human pose anomaly detection. In *Proceedings of the IEEE/CVF International Conference on Computer Vision*, pages 13545–13554, 2023. 2, 7, 8

[31] Chao Huang, Yabo Liu, Zheng Zhang, Chengliang Liu, Jie Wen, Yong Xu, and Yaowei Wang. Hierarchical graph embedded pose regularity learning via spatio-temporal transformer for abnormal behavior detection. In *Proceedings of the 30th ACM international conference on multimedia*, pages 307–315, 2022. 8

[32] Yashswi Jain, Ashvini Kumar Sharma, Rajbabu Velmurugan, and Biplab Banerjee. Posecvae: Anomalous human activity detection. In *2020 25th International Conference on Pattern Recognition (ICPR)*, pages 2927–2934. IEEE, 2021. 8

[33] Eric Jang, Shixiang Gu, and Ben Poole. Categorical reparameterization with gumbel-softmax. In *International Conference on Learning Representations*, 2017. 3, 4

[34] Sungjun Jang, Heansung Lee, Woo Jin Kim, Jungho Lee, Sungmin Woo, and Sangyoun Lee. Multi-scale structural graph convolutional network for skeleton-based action recognition. *IEEE Transactions on Circuits and Systems for Video Technology*, 2024. 6, 8

[35] QiuHong Ke, Mohammed Bennamoun, Senjian An, Ferdous Sohel, and Farid Boussaid. Learning clip representations for skeleton-based 3d action recognition. *IEEE Transactions on Image Processing*, 27(6):2842–2855, 2018. 8

[36] Jacob Devlin Ming-Wei Chang Kenton and Lee Kristina Toutanova. Bert: Pre-training of deep bidirectional transformers for language understanding. In *Proceedings of naacl-HLT*, page 2. Minneapolis, Minnesota, 2019. 2

[37] Alex Khang, Vugar Abdullayev, Eugenia Litvinova, Svetlana Chumachenko, Abuzarova Vusala Alyar, and PTN Anh. Application of computer vision (cv) in the healthcare ecosystem. In *Computer Vision and AI-Integrated IoT Technologies in the Medical Ecosystem*, pages 1–16. CRC Press, 2024. 2

[38] Prannay Khosla, Piotr Teterwak, Chen Wang, Aaron Sarna, Yonglong Tian, Phillip Isola, Aaron Maschinot, Ce Liu, and Dilip Krishnan. Supervised contrastive learning. *Advances in neural information processing systems*, 33:18661–18673, 2020. 6, 1

[39] Alexander Kirillov, Eric Mintun, Nikhila Ravi, Hanzi Mao, Paul Rolland, Laura Gustafson, Tete Xiao, Spencer Whitehead, Alexander C. Berg, et al. Segment anything. *arXiv preprint arXiv:2304.02643*, 2023. 3

[40] Muhammed Kocabas, Salih Karagoz, and Emre Akbas. Self-supervised learning of 3d human pose using multi-view geometry. In *Proceedings of the IEEE/CVF conference on computer vision and pattern recognition*, pages 1077–1086, 2019. 2

[41] Jiefeng Li, Can Wang, Hao Zhu, Yihuan Mao, Hao-Shu Fang, and Cewu Lu. Crowdpose: Efficient crowded scenes pose estimation and a new benchmark. In *Proceedings of the IEEE/CVF conference on computer vision and pattern recognition*, pages 10863–10872, 2019. 7

[42] Linguo Li, Minsi Wang, Bingbing Ni, Hang Wang, Jiancheng Yang, and Wenjun Zhang. 3d human action representation learning via cross-view consistency pursuit. In *2021 IEEE/CVF Conference on Computer Vision and Pattern Recognition (CVPR)*, pages 4739–4748, 2021. 6

[43] Maosen Li, Siheng Chen, Xu Chen, Ya Zhang, Yanfeng Wang, and Qi Tian. Actional-structural graph convolutional networks for skeleton-based action recognition. In *Proceedings of the IEEE/CVF conference on computer vision and pattern recognition*, pages 3595–3603, 2019. [6](#), [8](#)

[44] Shuai Li, Wanqing Li, Chris Cook, Ce Zhu, and Yanbo Gao. Independently recurrent neural network (indrnn): Building a longer and deeper rnn. In *Proceedings of the IEEE conference on computer vision and pattern recognition*, pages 5457–5466, 2018. [6](#)

[45] K. Lin, L. Wang, and Z. Liu. Mesh graphomer. In *2021 IEEE/CVF International Conference on Computer Vision (ICCV)*, pages 12919–12928, Los Alamitos, CA, USA, 2021. IEEE Computer Society. [2](#)

[46] Jun Liu, Amir Shahroudy, Dong Xu, and Gang Wang. Spatio-temporal lstm with trust gates for 3d human action recognition. In *Computer Vision–ECCV 2016: 14th European Conference, Amsterdam, The Netherlands, October 11–14, 2016, Proceedings, Part III 14*, pages 816–833. Springer, 2016. [6](#), [8](#)

[47] Jun Liu, Amir Shahroudy, Dong Xu, Alex C Kot, and Gang Wang. Skeleton-based action recognition using spatio-temporal lstm network with trust gates. *IEEE transactions on pattern analysis and machine intelligence*, 40(12):3007–3021, 2017. [8](#)

[48] Jun Liu, Gang Wang, Ping Hu, Ling-Yu Duan, and Alex C. Kot. Global context-aware attention lstm networks for 3d action recognition. In *2017 IEEE Conference on Computer Vision and Pattern Recognition (CVPR)*, pages 3671–3680, 2017. [8](#)

[49] Jun Liu, Gang Wang, Ping Hu, Ling-Yu Duan, and Alex C. Kot. Global context-aware attention lstm networks for 3d action recognition. In *Proceedings of the IEEE conference on computer vision and pattern recognition*, pages 1647–1656, 2017. [8](#)

[50] Jun Liu, Amir Shahroudy, Mauricio Perez, Gang Wang, Ling-Yu Duan, and Alex C Kot. Ntu rgb+ d 120: A large-scale benchmark for 3d human activity understanding. *IEEE transactions on pattern analysis and machine intelligence*, 42(10):2684–2701, 2019. [8](#)

[51] Jun Liu, Amir Shahroudy, Mauricio Perez, Gang Wang, Ling-Yu Duan, and Alex C. Kot. Ntu rgb+d 120: A large-scale benchmark for 3d human activity understanding. *IEEE Trans. Pattern Anal. Mach. Intell.*, 42(10): 2684–2701, 2020. [6](#), [8](#), [1](#)

[52] Wen Liu, Weixin Luo, Dongze Lian, and Shenghua Gao. Future frame prediction for anomaly detection – a new baseline. In *Proceedings of the IEEE Conference on Computer Vision and Pattern Recognition (CVPR)*, 2018. [8](#)

[53] Wen Liu, Weixin Luo, Dongze Lian, and Shenghua Gao. Future frame prediction for anomaly detection—a new baseline. In *Proceedings of the IEEE conference on computer vision and pattern recognition*, pages 6536–6545, 2018. [7](#), [8](#), [1](#)

[54] Yang Liu, Dingkang Yang, Yan Wang, Jing Liu, Jun Liu, Azzedine Boukerche, Peng Sun, and Liang Song. Generalized video anomaly event detection: Systematic taxonomy and comparison of deep models. 56(7), 2024. [7](#)

[55] Ziyu Liu, Hongwen Zhang, Zhenghao Chen, Zhiyong Wang, and Wanli Ouyang. Disentangling and unifying graph convolutions for skeleton-based action recognition. In *2020 IEEE/CVF Conference on Computer Vision and Pattern Recognition (CVPR)*, pages 140–149, 2020. [6](#), [8](#)

[56] Ziyu Liu, Hongwen Zhang, Zhenghao Chen, Zhiyong Wang, and Wanli Ouyang. Disentangling and unifying graph convolutions for skeleton-based action recognition. In *Proceedings of the IEEE/CVF conference on computer vision and pattern recognition*, pages 143–152, 2020. [8](#)

[57] Kui Luo, Xuan Kong, Jie Zhang, Jie Xu, Jinzhao Li, and Hao Tang. Computer vision-based bridge inspection and monitoring: A review. *Sensors*, 23(18):7863, 2023. [2](#)

[58] Weixin Luo, Wen Liu, and Shenghua Gao. A revisit of sparse coding based anomaly detection in stacked rnn framework. In *Proceedings of the IEEE International Conference on Computer Vision (ICCV)*, 2017. [8](#)

[59] Zhengxiong Luo, Zhicheng Wang, Yan Huang, Liang Wang, Tieniu Tan, and Erjin Zhou. Rethinking the heatmap regression for bottom-up human pose estimation. In *Proceedings of the IEEE/CVF conference on computer vision and pattern recognition*, pages 13264–13273, 2021. [2](#)

[60] Zixian Ma, Jerry Hong, Mustafa Omer Gul, Mona Gandhi, Irena Gao, and Ranjay Krishna. Crepe: Can vision-language foundation models reason compositionally? In *Proceedings of the IEEE/CVF Conference on Computer Vision and Pattern Recognition*, pages 10910–10921, 2023. [2](#)

[61] Amir Markovitz, Gilad Sharir, Itamar Friedman, Lihai Zelnik-Manor, and Shai Avidan. Graph embedded pose clustering for anomaly detection. In *Proceedings of the IEEE/CVF Conference on Computer Vision and Pattern Recognition*, pages 10539–10547, 2020. [7](#), [8](#)

[62] Raphael Memmesheimer, Nick Theisen, and Dietrich Paulus. Sl-dml: Signal level deep metric learning for multimodal one-shot action recognition. In *2020 25th International conference on pattern recognition (ICPR)*, pages 4573–4580. IEEE, 2021. [8](#)

[63] Raphael Memmesheimer, Simon Häring, Nick Theisen, and Dietrich Paulus. Skeleton-dml: Deep metric learning for skeleton-based one-shot action recognition. In *Proceedings of the IEEE/CVF Winter Conference on Applications of Computer Vision*, pages 3702–3710, 2022. [8](#)

[64] Shuangyan Miao, Yonghong Hou, Zhimin Gao, Mingliang Xu, and Wanqing Li. A central difference graph convolutional operator for skeleton-based action recognition. *IEEE Transactions on Circuits and Systems for Video Technology*, 32(7):4893–4899, 2021. [6](#), [8](#)

[65] Romero Morais, Vuong Le, Truyen Tran, Budhadiya Saha, Moussa Mansour, and Svetha Venkatesh. Learning regularity in skeleton trajectories for anomaly detection in videos. In *Proceedings of the IEEE/CVF conference on computer vision and pattern recognition*, pages 11996–12004, 2019. [7](#), [8](#), [1](#)

[66] Devon Myers, Rami Mohawesh, Venkata Ishwarya Chellaboina, Anantha Lakshmi Sathvik, Praveen Venkatesh, Yi-Hui Ho, Hanna Henshaw, Muna Alhawwreh, David Berdik, and Yaser Jararweh. Foundation

and large language models: fundamentals, challenges, opportunities, and social impacts. *Cluster Computing*, 27(1):1–26, 2024. 2, 3

[67] Christopher Neff, Matías Mendieta, Shrey Mohan, Mohammadmehdi Baharani, Samuel Rogers, and Hamed Tabkhi. Revamp 2 t: real-time edge video analytics for multicamera privacy-aware pedestrian tracking. *IEEE Internet of Things Journal*, 7(4):2591–2602, 2019. 2

[68] Ghazal Alinezhad Noghre, Armin Danesh Pazho, and Hamed Tabkhi. An exploratory study on human-centric video anomaly detection through variational autoencoders and trajectory prediction. In *Proceedings of the IEEE/CVF Winter Conference on Applications of Computer Vision (WACV) Workshops*, pages 995–1004, 2024. 8

[69] Ghazal Alinezhad Noghre, Armin Danesh Pazho, and Hamed Tabkhi. An exploratory study on human-centric video anomaly detection through variational autoencoders and trajectory prediction. In *Proceedings of the IEEE/CVF Winter Conference on Applications of Computer Vision*, pages 995–1004, 2024. 2

[70] Georgios Pavlakos, Xiaowei Zhou, and Kostas Daniilidis. Ordinal depth supervision for 3d human pose estimation. In *2018 IEEE/CVF Conference on Computer Vision and Pattern Recognition*, pages 7307–7316, 2018. 2

[71] Armin Danesh Pazho, Christopher Neff, Ghazal Alinezhad Noghre, Babak Rahimi Ardabili, Shanle Yao, Mohammadmehdi Baharani, and Hamed Tabkhi. Ancilia: Scalable intelligent video surveillance for the artificial intelligence of things. *IEEE Internet of Things Journal*, 10(17):14940–14951, 2023. 2

[72] Aditya Ramesh, Mikhail Pavlov, Gabriel Goh, Scott Gray, Chelsea Voss, Alec Radford, Mark Chen, and Ilya Sutskever. Zero-shot text-to-image generation. In *Proceedings of the 38th International Conference on Machine Learning*, pages 8821–8831. PMLR, 2021. 3, 4

[73] Hanoona Rasheed, Muhammad Uzair Khattak, Muhammad Maaz, Salman Khan, and Fahad Shahbaz Khan. Fine-tuned clip models are efficient video learners. In *Proceedings of the IEEE/CVF Conference on Computer Vision and Pattern Recognition*, pages 6545–6554, 2023. 2

[74] Ali Razavi, Aäron van den Oord, and Oriol Vinyals. *Generating diverse high-fidelity images with VQ-VAE-2*. Curran Associates Inc., Red Hook, NY, USA, 2019. 3

[75] Royston Rodrigues, Neha Bhargava, Rajbabu Velmurugan, and Subhasis Chaudhuri. Multi-timescale trajectory prediction for abnormal human activity detection. In *Proceedings of the IEEE/CVF winter conference on applications of computer vision*, pages 2626–2634, 2020. 7, 8

[76] Alberto Sabater, Laura Santos, Jose Santos-Victor, Alexandre Bernardino, Luis Montesano, and Ana C Murillo. One-shot action recognition in challenging therapy scenarios. In *Proceedings of the IEEE/CVF conference on computer vision and pattern recognition*, pages 2777–2785, 2021. 8

[77] István Sárándi, Timm Linder, Kai O. Arras, and Bastian Leibe. MeTRAbs: metric-scale truncation-robust heatmaps for absolute 3D human pose estimation. *IEEE Transactions on Biometrics, Behavior, and Identity Science*, 3(1):16–30, 2021. 2

[78] A. Shahroudy, J. Liu, T. Ng, and G. Wang. Ntu rgb+d: A large scale dataset for 3d human activity analysis. In *2016 IEEE Conference on Computer Vision and Pattern Recognition (CVPR)*, pages 1010–1019, Los Alamitos, CA, USA, 2016. IEEE Computer Society. 6, 8, 1

[79] Lei Shi, Yifan Zhang, Jian Cheng, and Hanqing Lu. Skeleton-based action recognition with directed graph neural networks. In *Proceedings of the IEEE/CVF conference on computer vision and pattern recognition*, pages 7912–7921, 2019. 6

[80] Lei Shi, Yifan Zhang, Jian Cheng, and Hanqing Lu. Two-stream adaptive graph convolutional networks for skeleton-based action recognition. In *Proceedings of the IEEE/CVF conference on computer vision and pattern recognition*, pages 12026–12035, 2019. 2, 6, 8

[81] L. Shi, Y. Zhang, J. Cheng, and H. Lu. Two-stream adaptive graph convolutional networks for skeleton-based action recognition. In *2019 IEEE/CVF Conference on Computer Vision and Pattern Recognition (CVPR)*, pages 12018–12027, Los Alamitos, CA, USA, 2019. IEEE Computer Society. 6

[82] Yi-Fan Song, Zhang Zhang, Caifeng Shan, and Liang Wang. Richly activated graph convolutional network for robust skeleton-based action recognition. *IEEE Transactions on Circuits and Systems for Video Technology*, 31(5):1915–1925, 2020. 6, 8

[83] Tae Soo Kim and Austin Reiter. Interpretable 3d human action analysis with temporal convolutional networks. In *Proceedings of the IEEE conference on computer vision and pattern recognition workshops*, pages 20–28, 2017. 6

[84] Yukun Su, Guosheng Lin, and Qingyao Wu. Self-supervised 3d skeleton action representation learning with motion consistency and continuity. In *2021 IEEE/CVF International Conference on Computer Vision (ICCV)*, pages 13308–13318, 2021. 6

[85] Ke Sun, Bin Xiao, Dong Liu, and Jingdong Wang. Deep high-resolution representation learning for human pose estimation. In *2019 IEEE/CVF Conference on Computer Vision and Pattern Recognition (CVPR)*, pages 5686–5696, 2019. 6

[86] Ke Sun, Bin Xiao, Dong Liu, and Jingdong Wang. Deep high-resolution representation learning for human pose estimation. In *Proceedings of the IEEE/CVF conference on computer vision and pattern recognition*, pages 5693–5703, 2019. 2

[87] Arash Vahdat, Evgeny Andriyash, and William Macready. Dvae#: Discrete variational autoencoders with relaxed boltzmann priors. *Advances in Neural Information Processing Systems*, 31, 2018. 2

[88] Arash Vahdat, William Macready, Zhengbing Bian, Amir Khoshman, and Evgeny Andriyash. Dvae++: Discrete variational autoencoders with overlapping transformations. In *International conference on machine learning*, pages 5035–5044. PMLR, 2018. 2

[89] Aaron van den Oord, Oriol Vinyals, and Koray Kavukcuoglu. Neural discrete representation learning. In *Proceedings of the 31st International Conference on*

Neural Information Processing Systems, page 6309–6318, Red Hook, NY, USA, 2017. Curran Associates Inc. 3

[90] Ashish Vaswani, Noam Shazeer, Niki Parmar, Jakob Uszkoreit, Llion Jones, Aidan N. Gomez, Łukasz Kaiser, and Illia Polosukhin. Attention is all you need. In *Proceedings of the 31st International Conference on Neural Information Processing Systems*, page 6000–6010, Red Hook, NY, USA, 2017. Curran Associates Inc. 5

[91] Ashish Vaswani, Noam Shazeer, Niki Parmar, Jakob Uszkoreit, Llion Jones, Aidan N. Gomez, Łukasz Kaiser, and Illia Polosukhin. Attention is all you need. In *Advances in Neural Information Processing Systems*, pages 5998–6008, 2017. 3

[92] Raviteja Vemulapalli, Felipe Arrate, and Rama Chellappa. Human action recognition by representing 3d skeletons as points in a lie group. In *Proceedings of the IEEE conference on computer vision and pattern recognition*, pages 588–595, 2014. 6

[93] Guodong Wang, Yunhong Wang, Jie Qin, Dongming Zhang, Xiuguo Bao, and Di Huang. Video anomaly detection by solving decoupled spatio-temporal jigsaw puzzles. In *Computer Vision – ECCV 2022*, pages 494–511, Cham, 2022. Springer Nature Switzerland. 7

[94] Haoxiang Wang, Pavan Kumar Anasosalu Vasu, Fartash Faghri, Raviteja Vemulapalli, Mehrdad Farajtabar, Sachin Mehta, Mohammad Rastegari, Oncel Tuzel, and Hadi Pouransari. Sam-clip: Merging vision foundation models towards semantic and spatial understanding. In *Proceedings of the IEEE/CVF Conference on Computer Vision and Pattern Recognition*, pages 3635–3647, 2024. 2

[95] Lei Wang and Piotr Koniusz. Temporal-viewpoint transportation plan for skeletal few-shot action recognition. In *Proceedings of the Asian Conference on Computer Vision*, pages 4176–4193, 2022. 8

[96] Lei Wang and Piotr Koniusz. Uncertainty-dtw for time series and sequences. In *European Conference on Computer Vision*, pages 176–195. Springer, 2022. 8

[97] Le Wang, Junwen Tian, Sanping Zhou, Haoyue Shi, and Gang Hua. Memory-augmented appearance-motion network for video anomaly detection. *Pattern Recognition*, 138:109335, 2023. 2, 8

[98] Wenhui Wang, Jifeng Dai, Zhe Chen, Zhenhang Huang, Zhiqi Li, Xizhou Zhu, Xiaowei Hu, Tong Lu, Lewei Lu, Hongsheng Li, et al. Internimage: Exploring large-scale vision foundation models with deformable convolutions. In *Proceedings of the IEEE/CVF conference on computer vision and pattern recognition*, pages 14408–14419, 2023. 2

[99] Tom Wehrbein, Marco Rudolph, Bodo Rosenhahn, and Bastian Wandt. Probabilistic monocular 3d human pose estimation with normalizing flows. In *2021 IEEE/CVF International Conference on Computer Vision (ICCV)*, pages 11179–11188, 2021. 2

[100] Cong Wu, Xiao-Jun Wu, and Josef Kittler. Graph2net: Perceptually-enriched graph learning for skeleton-based action recognition. *IEEE transactions on circuits and systems for video technology*, 32(4):2120–2132, 2021. 8

[101] Rongjie Xia, Yanshan Li, and Wenhan Luo. Laga-net: Local-and-global attention network for skeleton based action recognition. *IEEE Transactions on Multimedia*, 24:2648–2661, 2021. 6, 8

[102] Jianyang Xie, Yanda Meng, Yitian Zhao, Anh Nguyen, Xiaoyun Yang, and Yalin Zheng. Dynamic semantic-based spatial graph convolution network for skeleton-based human action recognition. In *Proceedings of the AAAI Conference on Artificial Intelligence*, pages 6225–6233, 2024. 2

[103] Tianhan Xu and Wataru Takano. Graph stacked hourglass networks for 3d human pose estimation. In *2021 IEEE/CVF Conference on Computer Vision and Pattern Recognition (CVPR)*, pages 16100–16109, 2021. 2

[104] Sijie Yan, Yuanjun Xiong, and Dahua Lin. Spatial temporal graph convolutional networks for skeleton-based action recognition. In *Proceedings of the Thirty-Second AAAI Conference on Artificial Intelligence and Thirtieth Innovative Applications of Artificial Intelligence Conference and Eighth AAAI Symposium on Educational Advances in Artificial Intelligence*. AAAI Press, 2018. 6, 8

[105] Sijie Yan, Yuanjun Xiong, and Dahua Lin. Spatial temporal graph convolutional networks for skeleton-based action recognition. In *Proceedings of the AAAI conference on artificial intelligence*, 2018. 2, 8

[106] Di Yang, Yaohui Wang, Antitza Dantcheva, Lorenzo Garattoni, Gianpiero Francesca, and Francois Bremond. Unik: A unified framework for real-world skeleton-based action recognition. *BMVC*, 2021. 2

[107] Siyuan Yang, Jun Liu, Shijian Lu, Meng Hwa Er, and Alex C Kot. Skeleton cloud colorization for unsupervised 3d action representation learning. In *Proceedings of the IEEE/CVF International Conference on Computer Vision*, pages 13423–13433, 2021. 6

[108] Siyuan Yang, Jun Liu, Shijian Lu, Er Meng Hwa, and Alex C Kot. One-shot action recognition via multi-scale spatial-temporal skeleton matching. *IEEE Transactions on Pattern Analysis and Machine Intelligence*, 2024. 2

[109] Shoubin Yu, Zhongyin Zhao, Haoshu Fang, Andong Deng, Haisheng Su, Dongliang Wang, Weihao Gan, Cewu Lu, and Wei Wu. Regularity learning via explicit distribution modeling for skeletal video anomaly detection. *IEEE Transactions on Circuits and Systems for Video Technology*, 2023. 7

[110] M Zaigham Zaheer, Arif Mahmood, M Haris Khan, Mattia Segu, Fisher Yu, and Seung-Ik Lee. Generative cooperative learning for unsupervised video anomaly detection. In *Proceedings of the IEEE/CVF conference on computer vision and pattern recognition*, pages 14744–14754, 2022. 2, 8

[111] Xianlin Zeng, Yalong Jiang, Wenrui Ding, Hongguang Li, Yafeng Hao, and Zifeng Qiu. A hierarchical spatio-temporal graph convolutional neural network for anomaly detection in videos. *IEEE Transactions on Circuits and Systems for Video Technology*, 33(1):200–212, 2021. 7

[112] Jinlu Zhang, Zhigang Tu, Jianyu Yang, Yujin Chen, and Junsong Yuan. Mixste: Seq2seq mixed spatio-temporal encoder for 3d human pose estimation in video. In *2022 IEEE/CVF Conference on Computer Vision and Pattern Recognition (CVPR)*, pages 13222–13232, 2022. 2

- [113] Pengfei Zhang, Cuiling Lan, Junliang Xing, Wenjun Zeng, Jianru Xue, and Nanning Zheng. View adaptive recurrent neural networks for high performance human action recognition from skeleton data. In *Proceedings of the IEEE international conference on computer vision*, pages 2117–2126, 2017. 6
- [114] Ce Zheng, Sijie Zhu, Matias Mendieta, Taojiannan Yang, Chen Chen, and Zhengming Ding. 3d human pose estimation with spatial and temporal transformers. *Proceedings of the IEEE International Conference on Computer Vision (ICCV)*, 2021. 2
- [115] Xingyi Zhou, Qixing Huang, Xiao Sun, Xiangyang Xue, and Yichen Wei. Towards 3d human pose estimation in the wild: A weakly-supervised approach. In *2017 IEEE International Conference on Computer Vision (ICCV)*, pages 398–407, 2017. 2
- [116] Anqi Zhu, QiuHong Ke, Mingming Gong, and James Bailey. Adaptive local-component-aware graph convolutional network for one-shot skeleton-based action recognition. In *Proceedings of the IEEE/CVF Winter Conference on Applications of Computer Vision*, pages 6038–6047, 2023. 8

MoFM: A Large-Scale Human Motion Foundation Model

Supplementary Material

7. Experimental Setup Details

7.1. Hyperparameters for DT1: Action Classification

As discussed in Section 5.1, we evaluate MoFM on NTU-RGB+D [78] (60 classes) and NTU-RGB+D-120 [51] (120 classes) for action recognition. The detailed hyperparameters for training on both datasets are presented in Table 6.

Table 6. Fine-tuning setup details for action classification on NTU-RGB+D [78] and NTU-RGB+D-120 [51] datasets.

Parameter	NTU-60	NTU-120
Epoch	16	20
Batch Size	24	
Optimizer	AdamW	
Adam β_1, β_2	0.9, 0.999	
Weight Decay	3e-4	
Base Learning Rate	1e-8	
Peak Learning Rate	1e-4	
Warmup Period	5 epochs	
Learning Rate Decay	Cosine	
Dropout	0.4	

7.2. Hyperparameters for DT2: One-shot Action Classification

We evaluate MoFM for one-shot action recognition on NTU-RGB+D-120 [51]. The model is trained on the auxiliary set (100 samples per class) using supervised contrastive learning [38], where $m = 2$ samples per class are randomly selected in each batch. Training hyperparameters are summarized in Table 7.

7.3. Hyperparameters for DT3: Self-supervised Human Anomaly Detection

As discussed in Section 5.3, we evaluate MoFM on the SHT [53] dataset and its human-centric subset HR-SHT [65] for anomaly detection. The training hyperparameters for both datasets are presented in Table 8. Please note that the hyperparameters remain the same for HR-SHT, as it is a subset of the SHT dataset. HR-SHT [65] uses the same training set but features a different test set, which focuses exclusively on human-related anomalies.

7.4. Hyperparameters for DT4: Supervised Human Anomaly Detection

As discussed in Section 5.4, for supervised anomaly detection we utilized the UBnormal dataset [2]. Detailed hyper-

Table 7. Fine-tuning setup details for one-shot action classification on NTU-RGB+D-120 [51] dataset.

Parameter	Value
Epoch	5
Batch Size	16
Optimizer	AdamW
Adam β_1, β_2	0.9, 0.999
Weight Decay	3e-4
Base Learning Rate	1.e-8
Peak Learning Rate	1.e-5
Warmup Period (Epochs)	0.3
Learning Rate Decay	Cosine
Dropout	0.4
Contrastive Temp	0.1

Table 8. Fine-tuning setup details for self-supervised anomaly detection on SHT [53] dataset.

Parameter	Value
Epoch	1
Batch Size	16
Optimizer	Adam
Adam β_1, β_2	0.9, 0.999
Weight Decay	6e-4
Base Learning Rate	1e-8
Peak Learning Rate	6e-4
Learning Rate Decay	OneCycleLR
Dropout	0.4

parameters for the fine-tuning process are provided in Table 9 to ensure reproducibility.

Table 9. Fine-tuning setup details for supervised anomaly detection on UBnormal [2] dataset.

Parameter	Value
Epoch	8
Batch Size	16
Optimizer	Adam
Adam β_1, β_2	0.9, 0.999
Weight Decay	3e-4
Base Learning Rate	1e-8
Peak Learning Rate	1e-4
Learning Rate Decay	OneCycleLR
Dropout	0.4